Diode junction temperature in ultraviolet AlGaN quantum-disks-in-nanowires

Diode junction temperature in ultraviolet AlGaN quantum-disks-in-nanowires

Davide Priante, Rami T. Elafandy, Aditya Prabaswara, Bilal Janjua, Chao Zhao, Mohd Sharizal Alias, Malleswararao Tangi, Yazeed Alaskar, Abdulrahman M. Albadri, Ahmed Y. Alyamani, Tien Khee Ng, and Boon S. Ooi

Citation: Journal of Applied Physics **124**, 015702 (2018); doi: 10.1063/1.5026650

View online: https://doi.org/10.1063/1.5026650

View Table of Contents: http://aip.scitation.org/toc/jap/124/1

Published by the American Institute of Physics

Diode junction temperature in ultraviolet AlGaN quantum-disks-in-nanowires

Davide Priante,[1] Rami T. Elafandy,[1] Aditya Prabaswara,[1] Bilal Janjua,[1] Chao Zhao,[1] Mohd Sharizal Alias,[1] Malleswararao Tangi,[1] Yazeed Alaskar,[2] Abdulrahman M. Albadri,[2] Ahmed Y. Alyamani,[2] Tien Khee Ng,[1,a)] and Boon S. Ooi[1,b)]

[1]*King Abdullah University of Science and Technology (KAUST), Photonics Laboratory, Thuwal 23955-6900, Saudi Arabia*

[2]*National Center for Nanotechnology, King Abdulaziz City for Science and Technology (KACST), Riyadh 11442-6086, Saudi Arabia*

(Received 22 February 2018; accepted 19 June 2018; published online 5 July 2018)

The diode junction temperature (T_j) of light emitting devices is a key parameter affecting the efficiency, output power, and reliability. Herein, we present experimental measurements of the T_j on ultraviolet (UV) AlGaN nanowire (NW) light emitting diodes (LEDs), grown on a thin metal-film and silicon substrate using the diode forward voltage and electroluminescence peak-shift methods. The forward-voltage vs temperature curves show temperature coefficient dV_F/dT values of −6.3 mV/°C and −5.2 mV/°C, respectively. The significantly smaller T_j of ∼61 °C is measured for the sample on the metal substrate, as compared to that of the sample on silicon (∼105 °C), at 50 mA, which results from the better electrical-to-optical energy conversion and the absence of the thermally insulating SiN_x at the NWs/silicon interface. In contrast to the reported higher T_j values for AlGaN planar LEDs exhibiting low lateral and vertical heat dissipation, we obtained a relatively lower T_j at similar values of injection current. Lower temperatures are also achieved using an Infrared camera, confirming that the T_j reaches higher values than the overall device temperature. Furthermore, the heat source density is simulated and compared to experimental data. This work provides insight into addressing the high junction temperature limitations in light-emitters, by using a highly conductive thin metal substrate, and it aims to realize UV AlGaN NWs for high power and reliable emitting devices. https://doi.org/10.1063/1.5026650

I. INTRODUCTION

III-nitride light emitters have emerged as attractive ultraviolet (UV) light sources owing to their environmentally friendly (mercury-free) material properties, high reliability, and cost-effectiveness. In particular, $Al_xGa_{1-x}N$ materials attracted attention due to their bandgap tunability throughout the UV range, hence allowing the use of this material in various electronic and optoelectronic applications.[1] Although high power AlGaN-based light emitting diodes (LEDs) have been well demonstrated with emission wavelength ranging from UV-A- to UV-C regions,[2–4] the device efficiency suffers from the detrimental thermal heating associated with the high operating current. LEDs usually operate at high injection current and most of these devices show such a decrease in efficiencies for current injections as low as 10 A/cm^2.[5] While some part of the electrical input power is converted into photons yielding the illumination, most of it remains within the device as heat, which is lost in Joule heating. Such a drop in efficiency is dominantly related to the diode junction temperature (T_j) that can reach values higher than the ambient operating temperatures and the overall device temperature. The increment in T_j not only affects the device efficiency, but also the operating voltage, emission wavelength,[6,7] power output,[8] chromaticity, and reliability.[9] Specifically, prolonged current injection leads to higher T_j which drastically degrades the LED performance, thereby causing catastrophic device failure. Various methods have been employed for measuring the junction temperature such as Raman spectroscopy,[10] thermal resistance,[11] photoluminescence,[12] nematic liquid crystals,[13] electroluminescence (EL) (band peak shift and high-energy slope of the spectrum),[14] and diode forward voltage.[15] Among these, the forward voltage method is considered the most accurate, though a precise calibration is needed for each device under test.

III-nitride nanowires (NWs) have attracted much interest as they circumvent planar device problems such as strain-induced polarization, threading dislocation, and cost-effective growth on various substrates. While NWs on a silicon substrate consist of a desirable platform for low-cost and scalable devices, the spontaneous formation of the insulating SiN_x layer at the semiconductor/substrate interface limits their applicability, impeding heat dissipation and electrical conduction.[16] It has been recently demonstrated that the NW growth on metal thin films helps to avoid such issues, hence reducing the potential barrier for carrier flow and allowing increased current injections with lower Joule heating.[17–21]

As many efforts have been made in the UV III-nitride NW community to bring NW technology to a practical application, it is of particular importance to study the diode T_j of such devices to evaluate the best configuration for efficient heat dissipation through the heat sink substrate, prevent

a)tienkhee.ng@kaust.edu.sa
b)boon.ooi@kaust.edu.sa

overheating, short lifespan, and reduced light intensity. To date, there are no reports on UV AlGaN (and in general III-nitride) NWs LED T_j measurements; therefore, this work consists of experimental findings that aim to enlighten the UV LED NW community for designing and optimizing the diode structures and substrate and to realize high power and reliable devices for eventual practical implementation.

We present T_j measurements by employing the diode forward voltage and the energy peak-shift methods on UV $Al_xGa_{1-x}N/Al_yGa_{1-y}N$ quantum disk (QD)/quantum barrier ($x < y$) NW LEDs grown on metal (Ti/TaN) and silicon substrates. Despite the lower thermal conductivity of the metal template, we observed lower T_j of 61 °C as compared to that of Si (105 °C) at 50 mA. This reveals that the reduced T_j is mainly due to the more efficient electrical-to-optical energy conversion of the sample grown on the metal substrate and therefore reduced Joule heating. We have reported recently that AlGaN NWs grown on metal thin films can achieve higher injection current due to the increased electrical conductivity and the absence of the above-mentioned SiN_x barrier at the substrate/NW interface.[20] We report a lower T_j compared to planar UV GaN and AlGaN planar structures by using the same forward voltage method (compared to previous reports). Comparison of T_j using the EL peak-shift method and infrared (IR) thermo-camera resulted in slightly lower values as previously reported in planar devices.

II. EXPERIMENTAL

The $Al_xGa_{1-x}N/Al_yGa_{1-y}N$ NW devices are grown on Ti (80 nm)/TaN (20 nm)/Si (100) and on silicon substrates using the molecular beam epitaxy (MBE). The metal deposition, NW growth, and fabrication process details can be found in Refs. 20 and 22. Briefly, for the sample on metal, the growth was initiated with ~85 nm n-GaN followed by 50 nm n-AlGaN. The active region is composed of 10 stacked $Al_xGa_{1-x}N$ quantum disks (3 nm)/$Al_yGa_{1-y}N$ quantum barriers (4 nm), $x < y$. p^+-AlGaN contact layer is then grown above a p-AlGaN layer with a total thickness of 20 nm. For the sample on the silicon substrate, ~150 nm n-GaN is grown, followed by 75 nm n-AlGaN. 15 stacked $Al_xGa_{1-x}N/Al_yGa_{1-y}N$ quantum disks/quantum barriers are then grown atop the n-doped layer. The p-contact layer is formed growing 10 nm p-GaN. The samples are fabricated using the contact lithography technique. Ni (5 nm)/Au (5 nm) was evaporated and annealed to form an ohmic contact with p-AlGaN and subsequent Ni (10 nm)/Au (400 nm) and Ti (10 nm)/Au (150 nm) are deposited as p- and n-contacts, respectively.

For the calibration of the diode forward voltage method, a semi-automated probe system (Cascade Microtech Summit 11000 AP) was incorporated with a pulsed source meter (Keithley 2611B, 1% duty cycle, 25 ms pulses). The measurement of the instant voltage and the voltage at the equilibrium was performed using a direct-current (DC) source meter (Keithley 2400). The EL spectrum was collected using a 15× objective lens (Thorlabs LMU-15X-UVB, focal length 13 mm and numerical aperture (NA) of 0.32, with anti-reflection (AR) coating for the 240–360 nm wavelength range, and a 50:50 beam-splitter (Thorlabs BSW19, AR coated for 250–450 nm) to distribute the light to the focusing lenses of a viewing camera.

The viewing camera consists of an infrared (IR) camera (Infrasight IS640) incorporated with an uncooled amorphous silicon microbolometer with an array size of 640 × 480 pixels and a spectral response ranging from 7 to 14 μm.

III. RESULTS AND DISCUSSION

The diode forward voltage method is based on the Shockley diode equation[15]

$$J_F = J_S\left[e^{\left(\frac{eV_F}{nkT}\right)} - 1\right], \tag{1}$$

where J_F is the applied current density, J_S is the saturation current density, n is the ideality factor, V_F is the forward voltage, k is the Boltzmann constant, and T is the temperature. In order to obtain the relation between the voltage and the temperature (and considering $V_F \gg kT/e$), we need to rewrite Eq. (1) as[15]

$$V_F = \frac{nkT}{e}\ln\left(\frac{J_F}{J_S}\right). \tag{2}$$

And the change of junction voltage as a function of temperature can be expressed as[15]

$$\frac{dV_F}{dT} = \frac{d}{dT}\left[\frac{nkT}{e}\ln\left(\frac{J_F}{J_S}\right)\right]. \tag{3}$$

It is noted that the temperature dependence of junction voltage is due to the temperature dependence of intrinsic carrier concentration, effective densities of states in the conduction and valence bands, and material bandgap energy and that the contribution of the latter is approximately 24% for GaN.[23] Experimentally, with increasing temperature, the junction voltage decreases when working at constant current. Such linear dependence of V_F and T can be fitted as

$$V_F = \alpha + K_T T_O, \tag{4}$$

where K_T is the temperature coefficient and T_O is the temperature of the heat sink.

Figure 1(a) shows the I-V curve of the AlGaN NW LED on the metal and silicon substrate under DC operation. The turn-on voltages of the devices are ~8 and 10 V, respectively, while the turn-on resistances are ~14 and 80 Ω. During the calibration measurement of the AlGaN NWs on metal, the current was increased from 1 to 7 mA and the measured V_F versus T plot is shown in Fig. 1(b). The temperature coefficient, i.e., dV_F/dT, of −6.3 mV/°C is slightly lower than previously experimentally measured UV AlGaN and GaN planar LEDs of −5.8 mV/°C[14] and -2.3 mV/°C,[15] and lower than theoretical values (−1.76 mV/°C).[23] In fact, the latter defines the lower limit of the magnitude of dV_F/dT. Moreover, it does not take into account the contribution from the resistive-higher-doping-activation neutral regions at high temperatures, where the resistivity decreases together with the voltage. Figure 1(c) shows the V_F versus T plot for the

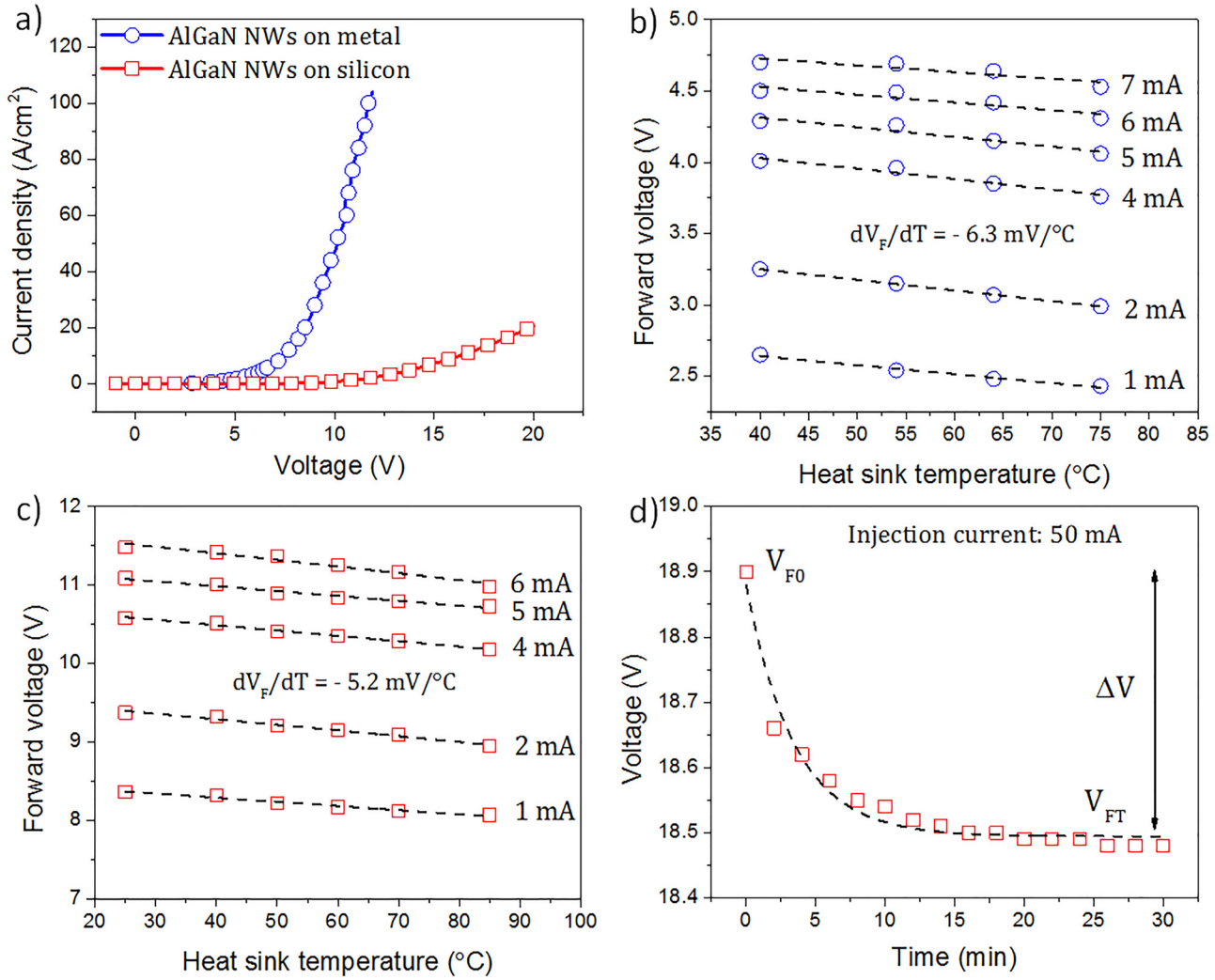

FIG. 1. Forward voltage method calibration. (a) I-V curve for the AlGaN NW LEDs on metal and silicon substrate under DC. (b) Forward voltage vs heat sink temperature for the AlGaN NWs LED on metal. (c) Forward voltage vs heat sink temperature for the AlGaN NWs LED on silicon, and (d) forward voltage variation as a function of time at 50 mA for the sample on silicon.

AlGaN NWs on the silicon substrate with a temperature coefficient of -5.2 mV/°C.

From Eq. (4), the junction temperature can be obtained as[24]

$$T_j = T_A + \frac{(V_{FT} - V_{FO})}{K_T}, \tag{5}$$

where T_A is the ambient temperature and V_{FT} and V_{FO} are the equilibrium and instant voltage.[24] An example of the V_{FT} at 50 mA (DC operation) at room temperature for the device on silicon is shown in Fig. 1(d). The V_{FT} is the constant forward voltage at thermal equilibrium, i.e., measured after 30 min at constant current. At thermal equilibrium, the voltage reaches a plateau. At 50 mA, the instant (initial) voltage is 18.90 V, while after equilibrium it is 18.48 V. The high voltage measured is a consequence of the high device resistance that is possibly due to the spontaneous SiN_x layer at the GaN/Si interface. The resultant ΔV is equal to 42 mV that is substantially higher than GaN-based planar devices. It is also noted that, as the current increases, the ΔV further increases.

In order to compare the results obtained using the forward voltage method, we measured the T_j using the EL emission peak-shift method. The band-gap-dependent temperature coefficient K_λ needs to be extracted and the T_j can be calculated as follows:[25]

$$T_j = T_O + \frac{\Delta\lambda}{K_\lambda}, \tag{6}$$

where T_O is the ambient temperature and $\Delta\lambda$ is the peak emission wavelength difference measured in DC and pulsed current. Figure 2(a) shows the emission peak shift as a function of temperature for the AlGaN NW LED on the metal substrate. Different devices were tested and an average K_λ of 0.027 nm/°C was calculated for a pulsed injection current of 90 mA. It is noted that K_λ did not change much with injection current, confirming that the duty cycle used is small enough to prevent the device from heating. Figure 2(b) depicts the EL spectrum in DC and pulsed mode at 90 mA for the sample on the metal substrate. The peak emission in the DC mode is at 324.97 nm, while in the pulsed mode it is at 324.74 nm, giving a $\Delta\lambda = 0.23$ nm. The slightly longer peak emission wavelength

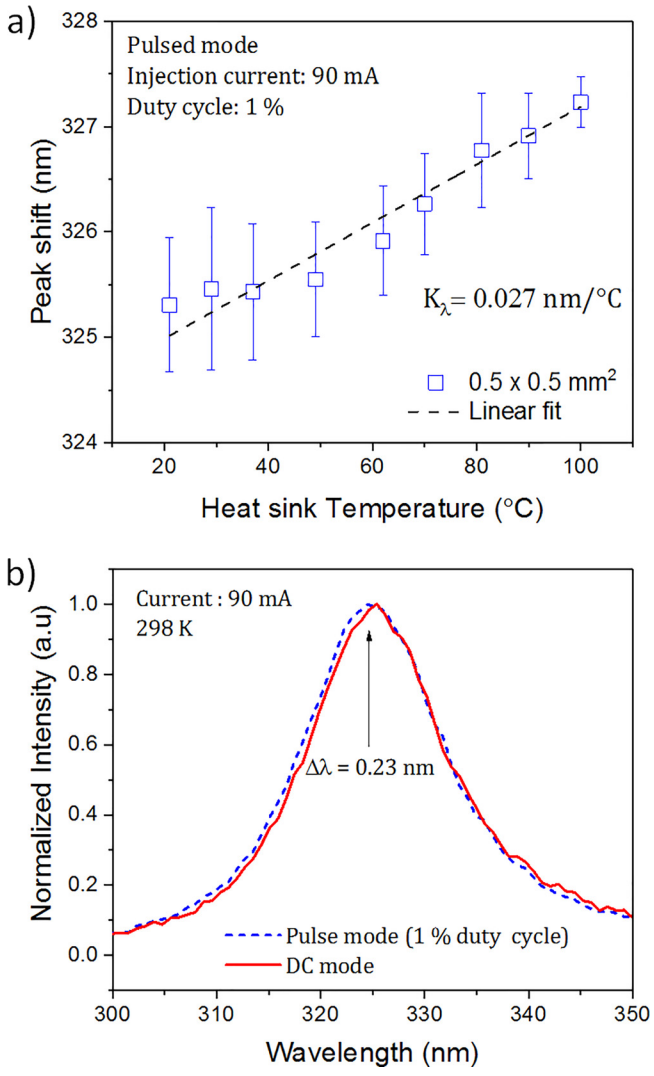

FIG. 2. EL peak-shift method calibration for the AlGaN NWs LED on metal substrate. (a) Peak wavelength shift as a function of heat sink temperature (b) Normalized EL intensity in DC and pulse modes at 90 mA.

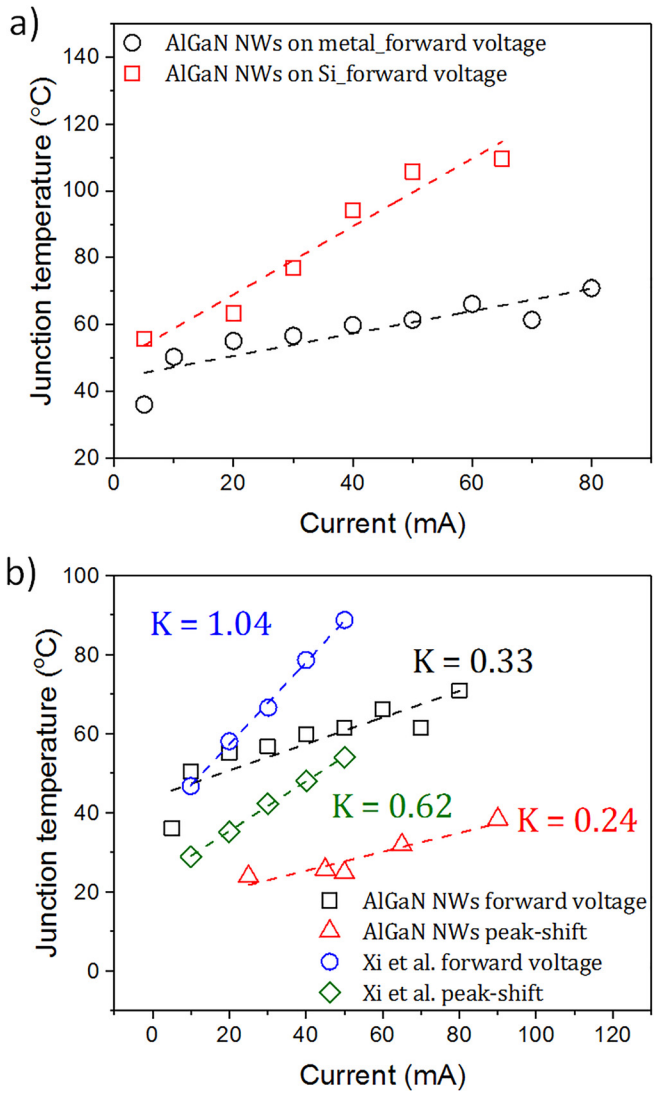

FIG. 3. T_j as a function of DC forward current. (a) Comparison between AlGaN NWs on the metal and silicon substrate using the forward voltage method. (b) Forward voltage method and EL peak-shift method comparison of AlGaN NWs on metal and AlGaN planar LED (Xi *et al.*).

in the DC mode is due to the device heating and internal bandgap reduction. The EL peak shift is more susceptible to effects of alloy-broadening and kT broadening, and it has been reported that the accuracy of the peak wavelength is ~10% of the EL full-width at half-maximum (FWHM).

The T_j comparison of the two samples, calculated using the forward voltage method, as a function of injection current, is shown in Fig. 3(a). Lower values are obtained for the NWs on the metal substrate. As the current increases from 5 to 80 mA, the T_j increases from 36 to 71 °C. On the other hand, the T_j for the NWs on silicon shows higher values. At 50 mA the T_j is ~105 °C, higher than that of the sample on metal, 61 °C. Moreover, the increment of T_j of the sample grown directly on silicon is steeper than that of the sample grown on metal, especially at elevated injection currents. This, however, cannot be explained by the thermal conductivity of the substrate as Ti (13–22 $W \cdot m^{-1} \cdot K^{-1}$)[26] has a thermal conductivity lower than silicon (50–149 $W \cdot m^{-1} \cdot K^{-1}$).[27] Instead, this is due to the better electrical-to-optical energy conversion. We recently demonstrated the growth of AlGaN NW LEDs on Ti/TaN/Si to circumvent the SiN_x formation and substrate delamination.[20] We reported a higher injection current density due to the reduction of Si interdiffusion in the metal layer. This reduces the potential barrier at the semiconductor/substrate interface, increasing the injection efficiency and reducing Joule heating. However, it is noted that the LEDs grown on the Si substrate have a larger active region compared to the one grown on metal and this may also contribute to an increase in T_j. In Fig. 6(b), by comparing the corresponding increase in temperature at different heat source densities (Q) for the LED on silicon with 10 and 15 quantum disk-stacks, it is found that temperature increases with active region thickness as there is a larger heating volume. Furthermore, by comparing the LEDs on silicon and metal with the same 10 quantum disk-stacks, the temperature also increases by a similar amount for that grown on silicon. Therefore, the temperature increase, which contributes to the rise in T_j, is due to both the increase in the active region thickness and the interface barrier at the nanowire-silicon interface.

Figure 3(b) reports a comparison between AlGaN planar[14] and AlGaN NWs T_j vs injection current using both the diode forward voltage and EL emission peak-shift method. The NW devices show lower T_j compared to the planar devices grown on sapphire. This can be explained by the heat dissipation through the metal substrate. In fact, it has been reported that the substrate plays a crucial role in the LED T_j. Blue InGaN LEDs on sapphire and silicon substrates have shown Tj of ∼80 °C and ∼65 °C, respectively, when operated at 50 mA.[28] Similarly, at 100 mA, T_j values of InGaN LEDs on both sapphire and GaN substrates were reported to be ∼204 °C and ∼83 °C, respectively,[5] confirming the higher heat conductance in GaN and silicon compared to sapphire. Table I lists a summary of the III-nitride planar LED T_j in the chronological order. Specifically, in the UV region, GaN LEDs emitting at 375 nm have shown a T_j of ∼75 °C at 50 mA,[15] whereas T_j of the AlGaN LED emitting at 295 nm has been reported to be ∼90 °C for the same injection current.[14] Figure 4 shows the T_j of the reported group-III nitride LEDs in the literature using the forward voltage and peak-shift methods. Despite the lack of reports for a proper comparison on UV AlGaN light emitters, the NW devices on the metal substrate show the lowest T_j values at similar injection current. All the curves in Fig. 3(b) are linear with current and K represents the speed with which the temperature increases. As it can be noticed, T_j in planar structures increases faster compared to the NW structure, with a K value of 1.04 in the forward voltage method and 0.62 for the EL peak-shift method, compared to K values of 0.33 and 0.24 for the AlGaN NWs. This can be explained by the lower lateral and vertical (through the substrate) heat dissipation for the planar devices. Moreover, the EL peak-shift method shows lower T_j in both samples. For similar reasons, the T_j of the AlGaN NW sample on silicon using the EL peak-shift method could not be measured. The EL emission was too weak and together with the high inhomogeneity of the emission, it impeded the clear peak distinction in DC and pulsed current, especially at low injection. Moreover, especially for nanowire-based devices, where the inhomogeneity is more prominent, the peak-shift method is expected to impose an even larger error. In this regard, Xi *et al*. reported a variation of the junction temperature of ±24 °C that, if taken into account, agrees well with the results obtained by the forward voltage method.[14]

The overall devices temperatures were then measured using an IR camera. Figure 5(a) shows the current-dependent IR images of the $0.5 \times 0.5\,mm^2$ devices on the metal and silicon substrate. At 10 mA, the Joule heating is negligible for both devices. However, the device on silicon heats up faster compared to the one on the metal substrate. If we compare the devices at 50 mA, we notice that the one on metal shows lower temperature on the device area and on the surrounding area. This means that the absence of SiN_x contributes to a better heat spreading across the substrate. The current vs. temperature plot is depicted in Fig. 5(b). We show that the two samples reach the same temperature of 45 °C at 60 mA

TABLE I. Summary of the reported planar group-III nitride LED junction temperatures.

Institution and year	Material system	Emission wavelength (nm)	Junction temperature (°C)	Current (mA)	Substrate	Method
Rensselaer Polytechnic Institute, 2004[15]	GaN	375	73	54	Sapphire	Forward voltage
Rensselaer Polytechnic Institute, 2005[14]	AlGaN	295	89	50	Sapphire	Forward voltage
Rensselaer Polytechnic Institute, 2005[14]	AlGaN	295	54	50	Sapphire	EL Peak-shift
Rensselaer Polytechnic Institute, 2005[14]	AlGaN	295	140	50	Sapphire	High energy slope
Samsung Advanced Institute of Technology, 2005[29]	InGaN	400	25	100	Sapphire	EL Peak-shift
Nanchang University, 2007[28]	InGaN	460	82	50	GaN	Forward voltage
Nanchang University, 2007[28]	InGaN	460	65	50	Silicon	Forward voltage
Kyung Hee University, 2010[24]	InGaN	450	32	40	Sapphire (150 μm)	Forward voltage
Kyung Hee University, 2011[25]	InGaN	450	25	40	Sapphire	Forward voltage
National Taiwan Normal University, 2011[30]	InGaN	470	51	50	Sapphire	EL Peak-shift
Chang Gung University, 2012[31]	InGaN	521.4–506.9	16	50	Sapphire	Forward voltage
Chang Gung University, 2012[31]	InGaN	521.4–506.9	34	50	Sapphire	EL Peak-shift
Chang Gung University, 2012[31]	InGaN	521.4–506.9	82	50	Sapphire	High energy slope
Chonbuk National University, 2015[32]	InGaN	440	54	40	Graphene oxide/sapphire	Forward voltage
Chonbuk National University, 2017[33]	InGaN	440	30	135	Sapphire lift-off	Forward voltage
KAUST (Our work)	AlGaN NWs	325	61	50	Ti/TaN/Si	Forward voltage
KAUST (Our work)	AlGaN NWs	325	24	50	Ti/TaN/Si	EL Peak-shift

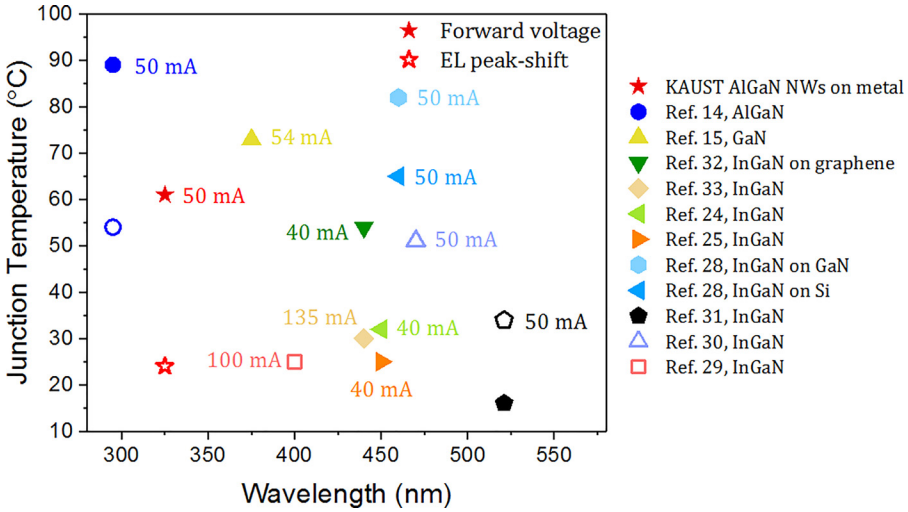

FIG. 4. T_j vs. wavelength/current plot for the reported group-III nitride LEDs, using the forward voltage and peak-shift method. The substrate is sapphire where not specified.

(sample on silicon) and 110 mA (sample on the metal). These temperatures are lower compared to the ones obtained using the forward voltage method, meaning that the T_j can reach values much higher than the overall device temperature. In fact, the IR camera measures the overall heating escaping the device under test. We also show the temperature curves for 1×1 and $2 \times 2\,mm^2$ devices on the metal. At low injection currents, the different size does not play a prominent role in the Joule heating across the device. However, for high current (80 mA), the temperature starts deviating due to the reduced current density with the increased device area.

To study the heat transfer across the device, we simulated the AlGaN NW LED on metal and silicon substrates using the finite element method (FEM) (COMSOL Multiphysics software). The heat source is generated in the active region and is dissipated by conduction through the substrate and by convection and radiation through the contact pads. The bottom of the NW LED is in contact with a heat sink kept at RT. The heat transfer was modeled by using the following 3D steady-state heat equations

$$\nabla \cdot (k\nabla T) = Q, \tag{7}$$

$$k\nabla T = h\,(T_{amb} - T) + \varepsilon\sigma\left(T_{amb}^4 - T^4\right), \tag{8}$$

$$\nabla T = \frac{\partial T}{\partial r}\hat{r} + \frac{1}{r}\frac{\partial T}{\partial \phi}\hat{\phi} + \frac{\partial T}{\partial Z}\hat{z}, \tag{9}$$

where Q is the heat source density, k is the thermal conductivity, h is the convection heat transfer, T_{amb} and T are the ambient temperature and the NW temperature, ε is the surface emissivity, and σ is the Stefan-Boltzmann constant. Figure 6(a) shows the device schematic at a heat source density of 10^{14} W/m^3 for the sample grown on the metal substrate. As the heat convection and radiation in NWs are negligible, the higher temperature is reached at the contact pads and heat dissipates faster through the substrate. Figure 6(b) depicts the comparison of active region temperature at different heat source densities for both devices, and a comparison with a device on the silicon substrate with the same active region thickness of the device on metal. The inset shows the cross section heat dissipation of the device on metal substrate. A temperature of ~60 °C for the sample on the metal substrate was achieved for a heat source density of $\sim 3.2 \times 10^{14}$ W/m^3 that is the T_j value that we obtained for an injection current at 50 mA. On the other hand, for the sample on the silicon substrate, a temperature of ~100 °C was obtained for the same heat source density. To verify these results, we calculated the heat source density generated in the active region under DC operation by analyzing the experimentally measured power-current-voltage (L-I-V)

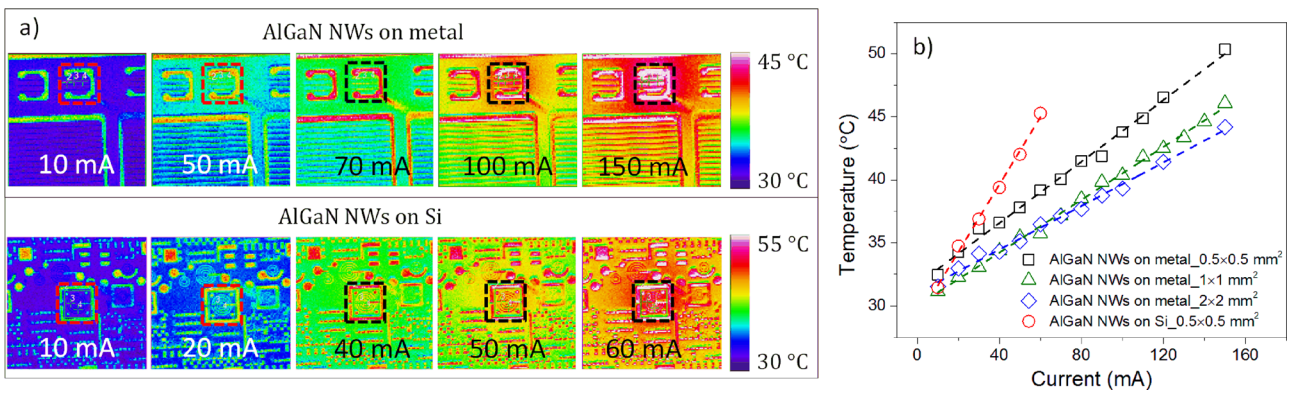

FIG. 5. (a) Infrared camera images at different currents of the $0.5 \times 0.5\,mm^2$ AlGaN NWs LEDs on metal and silicon substrate. (b) Temperature vs. current linear curves for different device areas.

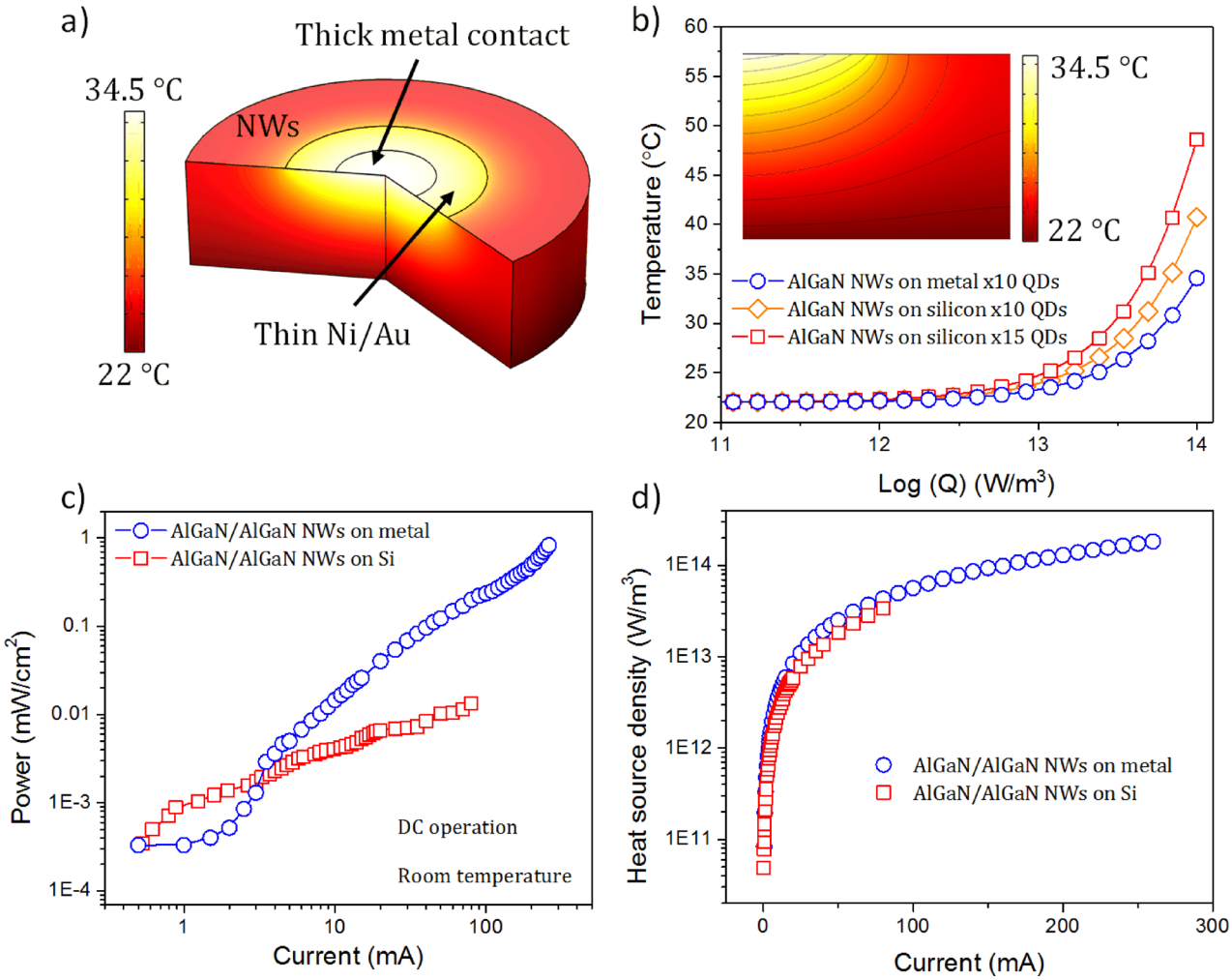

FIG. 6. (a) Temperature distribution in the NWs LED on metal substrate with a source heat density of 10^{14} W/m^3. (b) Simulated semilog plot of temperature vs. heat source density (Q) for the devices grown on metal and silicon substrates with 10 and 15 quantum disks-stack (QDs). The inset shows the contour cross section image of the device on metal. (c) Log-log L-I plot of AlGaN NW LEDs for samples on metal and silicon in DC operation. (d) Heat source density vs. current, calculated from (c) and Fig. 1(a).

characteristics. Figure 6(c) shows the log-log L-I curves for the AlGaN NWs on the metal and silicon substrate at room temperature. The heat source density can be calculated as[24]

$$Q = \frac{(I \cdot V - L)}{U_{QDisks}}, \tag{10}$$

where U_{QDisks} is the volume of the quantum disks.

Figure 6(d) represents the calculated heat source density with increasing current for the samples on the metal and silicon substrate. As expected, the Q values increased with injection current. At low injection, the heat source densities have similar values, while above ~20 mA the trends start deviating with the device on silicon showing slightly smaller values. This can be explained by the higher operating current of the sample on the metal substrate compared to the one on silicon that highly affects the heat source density calculation. Moreover, from Fig. 6(b), the two samples follow the same trend until $Q = \sim 10^{14}$ W/m^3, where the device on silicon starts deviating and the temperature increases. However, in the experimental results [Fig. 6(d)] the device on silicon does not reach a heat source density of 10^{14} W/m^3 as it cannot withstand such injection current. Hence, although we cannot experimentally verify it, simulation results indicate that after 10^{14} W/m^3 the Q value of the sample on the silicon substrate overcomes the one of metal. It is noted that the larger the thickness of the active region, the larger the temperature output at a given heat source density. From the experimental results, below ~10^{14} W/m^3 the heat source density for the sample on silicon is slightly lower compared to the one on metal, despite the larger number of quantum disks. Also, the junction temperature calculated using the forward voltage method shows higher values for the former, indicating that the thickness of the active region is not the only parameter affecting the temperature rise.

At 50 mA, the Q values were measured as 2.51×10^{13} W/m^3 and 1.8×10^{13} W/m^3, respectively, that are similar to that of the reported InGaN/GaN planar LEDs (~4.6×10^{13} W/m^3 at 60 mA).[24] These values, however, slightly differ from the simulated results obtained in Fig. 6(b), where for a heat source density of 2.51×10^{13} W/m^3 the temperature is ~26 °C that is lower than the expected 61 and 105 °C. This can be explained by the high thermal contact resistance caused by the rough surface between the device substrate

and the heat sink that leads to air pockets and causes a temperature drop across the interfaces.

IV. CONCLUSION

Junction temperature measurements are presented on the UV AlGaN NW LEDs on metal and silicon substrates. Reduced T_j measured using the forward voltage method was obtained for the device grown on a metal thin film with values ranging from 36–71 °C (5 to 80 mA) compared to 56–110 °C (5 to 65 mA) for the sample on the silicon substrate. The EL peak-shift method showed lower the T_j due to the larger error of the energy peak and FWHM of the EL spectra. A comparison with the previously reported AlGaN-based planar LED on sapphire showed that the AlGaN NW LED presents lower T_j that we assumed due to the better lateral and vertical heat dissipation as well as thermal conductivity of the metal substrate compared to sapphire. Measurements using the IR camera are also presented, confirming the reduced Joule heating and better heat dissipation for the LEDs grown on the metal substrate. Finite element method simulations were performed to study the heat transfer across the device and to understand the device temperature at specific active region heat source densities. This work aims to shed light on the uncharted heating problems in AlGaN NW light emitters on the Si substrate and presents a solution for eventual high power and reliable emitting devices on thin metal films.

ACKNOWLEDGMENTS

We acknowledge the financial support from the King Abdulaziz City for Science and Technology (KACST), Grant No. KACST TIC R2-FP-008. This work was partially supported by the King Abdullah University of Science and Technology (KAUST) baseline funding, No. BAS/1/1614-01-01 and MBE equipment funding No. C/M-20000-12-001-77.

[1]Y. Muramoto, M. Kimura, and S. Nouda, Semicond. Sci. Technol. **29**, 84004 (2014).
[2]S. Inoue, N. Tamari, and M. Taniguchi, Appl. Phys. Lett. **110**, 141106 (2017).
[3]T. Nishida, H. Saito, and N. Kobayashi, Appl. Phys. Lett. **79**, 711 (2001).
[4]A. J. Fischer, A. A. Allerman, M. H. Crawford, K. H. A. Bogart, S. R. Lee, R. J. Kaplar, W. W. Chow, S. R. Kurtz, K. W. Fullmer, and J. J. Figiel, Appl. Phys. Lett. **84**, 3394 (2004).
[5]J. Senawiratne, A. Chatterjee, T. Detchprohm, W. Zhao, Y. Li, M. Zhu, Y. Xia, X. Li, J. Plawsky, and C. Wetzel, Thin Solid Films **518**, 1732 (2010).
[6]Y. P. Varshni, Physica **34**, 149 (1967).
[7]P. Kraisingdecha and M. Gal, Appl. Phys. Lett. **69**, 1355 (1996).
[8]T. Egawa, H. Ishikawa, T. Jimbo, and M. Umeno, Appl. Phys. Lett. **69**, 830 (1996).
[9]S. Chhajed, Y. Xi, T. Gessmann, J.-Q. Xi, J. M. Shah, J. K. Kim, and E. F. Schubert, Proc. SPIE **5739**, 16–25 (2005).
[10]M. Kuball, J. W. Pomeroy, S. Rajasingam, A. Sarua, M. J. Uren, T. Martin, A. Lell, and V. Härle, Phys. Status Solidi **202**, 824 (2005).
[11]S. Murata and H. Nakada, J. Appl. Phys. **72**, 2514 (1992).
[12]D. C. Hall, L. Goldberg, and D. Mehuys, Appl. Phys. Lett. **61**, 384 (1992).
[13]J. Park, M. Shin, and C. C. Lee, Opt. Lett. **29**, 2656 (2004).
[14]Y. Xi, J.-Q. Xi, T. Gessmann, J. M. Shah, J. K. Kim, E. F. Schubert, A. J. Fischer, M. H. Crawford, K. H. A. Bogart, and A. A. Allerman, Appl. Phys. Lett. **86**, 31907 (2005).
[15]Y. Xi and E. F. Schubert, Appl. Phys. Lett. **85**, 2163 (2004).
[16]K. Hestroffer, C. Leclere, V. Cantelli, C. Bougerol, H. Renevier, and B. Daudin, Appl. Phys. Lett. **100**, 212107 (2012).
[17]B. Janjua, H. Sun, C. Zhao, D. H. Anjum, D. Priante, A. A. Alhamoud, A. M. Albadri, A. Y. Alyamani, M. M. El-desouki, T. N. Khee, and B. S. Ooi, Opt. Express **25**, 1381 (2017).
[18]M. Wolz, C. Hauswald, T. Flissikowski, T. Gotschke, S. Fernández-Garrido, O. Brandt, H. T. Grahn, L. Geelhaar, and H. Riechert, Nano Lett. **15**, 3743 (2015).
[19]A. T. M. Sarwar, S. D. Carnevale, F. Yang, T. F. Kent, J. J. Jamison, D. W. McComb, and R. C. Myers, Small **11**, 5402 (2015).
[20]D. Priante, B. Janjua, A. Prabaswara, R. C. Subedi, R. T. Elafandy, S. Lopatin, D. H. Anjum, C. Zhao, T. K. Ng, and B. S. Ooi, Opt. Mater. Express **7**, 4214 (2017).
[21]C. Zhao, T. K. Ng, R. T. ElAfandy, A. Prabaswara, G. B. Consiglio, I. A. Ajia, I. S. Roqan, B. Janjua, C. Shen, J. Eid, and others, Nano Lett. **16**, 4616 (2016).
[22]B. Janjua, H. Sun, C. Zhao, D. H. Anjum, F. Wu, A. A. Alhamoud, X. Li, A. M. Albadri, A. Y. Alyamani, M. M. El-Desouki, T. K. Ng, and B. S. Ooi, Nanoscale **9**, 7805 (2017).
[23]Y. Xi, T. Gessmann, J. Xi, J. K. Kim, J. M. Shah, E. F. Schubert, A. J. Fischer, M. H. Crawford, K. H. A. Bogart, and A. A. Allerman, Jpn. J. Appl. Phys., Part 1 **44**, 7260 (2005).
[24]H. K. Lee, J. S. Yu, and Y. T. Lee, Phys. Status Solidi **207**, 1497 (2010).
[25]D. H. Lee, H. K. Lee, J. S. Yu, S. J. Bae, J. H. Choi, D. H. Kim, I. C. Ju, K. M. Song, J. M. Kim, and C. S. Shin, Semicond. Sci. Technol. **26**, 55014 (2011).
[26]R. W. Powell and R. P. Tye, J. Less Common Met. **3**, 226 (1961).
[27]M. Mikulics, P. Kordoš, A. Fox, M. Kočan, H. Lüth, Z. Sofer, and H. Hardtdegen, Appl. Mater. Today **7**, 134 (2017).
[28]F. Jiang, W. Liu, Y. Li, W. Fang, C. Mo, M. Zhou, and H. Liu, J. Lumin. **122**, 693 (2007).
[29]J. Cho, C. Sone, Y. Park, and E. Yoon, Phys. Status Solidi **202**, 1869 (2005).
[30]Y.-J. Lee, C.-J. Lee, and C.-H. Chen, Jpn. J. Appl. Phys., Part 1 **50**, 04DG18 (2011).
[31]J.-C. Wang, C.-H. Fang, Y.-F. Wu, W.-J. Chen, D.-C. Kuo, P.-L. Fan, J.-A. Jiang, and T.-E. Nee, J. Lumin. **132**, 429 (2012).
[32]N. Han, E. Jung, M. Han, B. D. Ryu, K. B. Ko, Y. J. Park, T. Cuong, J. Cho, H. Kim, and C.-H. Hong, J. Phys. D: Appl. Phys. **48**, 265102 (2015).
[33]S. J. Oh and J. Cho, Thin Solid Films **641**, 8 (2017).